

Analysis of Maximum PowerPoint Tracking (MPPT) Adaptability in Inverters of the Three-Phase Photovoltaic Systems Integrated into the Electrical Grid of Congo-Brazzaville

Rostand Martialy Davy Loembe Souamy^{1,2,3,4,5*}, Mavie Grace Mimiessse¹,
Brel Levallois Ndzah Yombi², Zonzolo¹, Guoping Jiang³, Wanghong Hua⁴, Xubao Wen⁵

¹Laboratory of Electrical and Electronic Engineering (LGEE), National Higher Polytechnic School, Marien Ngouabi University, Brazzaville, Republic of the Congo

²National Institute of Research in Natural and Exact Sciences (IRSEN), Brazzaville, Republic of the Congo

³College of Automation and Artificial Intelligence, Nanjing University of Posts and Telecommunications, Nanjing, China

⁴Laboratory of Control Theory and Control Engineering, Hohai University College of Energy and Electrical Engineering, Nanjing, China

⁵Jiangsu Provincial Key Laboratory for Novel Technology, Department of Computers Sciences and Technology, Nanjing University, Nanjing, China

Email: *loembesouamy@gmail.com, lucianamimiessse@gmail.com

How to cite this paper: Souamy, R.M.D.L., Mimiessse, M.G., Yombi, B.L.N., Zonzolo, Jiang, G.P., Hua, W.H. and Wen, X.B. (2024) Analysis of Maximum PowerPoint Tracking (MPPT) Adaptability in Inverters of the Three-Phase Photovoltaic Systems Integrated into the Electrical Grid of Congo-Brazzaville. *Journal of Power and Energy Engineering*, **12**, 125-152.

<https://doi.org/10.4236/jpee.2024.1211008>

Received: October 24, 2024

Accepted: November 26, 2024

Published: November 29, 2024

Copyright © 2024 by author(s) and Scientific Research Publishing Inc.

This work is licensed under the Creative Commons Attribution International License (CC BY 4.0).

<http://creativecommons.org/licenses/by/4.0/>



Open Access

Abstract

This paper investigates the adaptability of Maximum Power Point Tracking (MPPT) algorithms in single-stage three-phase photovoltaic (PV) systems connected to the grid of Congo-Brazzaville and compares the attributes of various conventional, significance and novelty of controller system of the proposed of method and improved Incremental Conductance algorithms, Perturbation and Observation Techniques, and other Maximum Power Point Tracking (MPPT) algorithms in normal and partial shading conditions. Performance evaluation techniques are discussed on the basis of the dynamic parameters of the PV system although the control of this structure is relatively advanced technology but the conversion efficiency is difficult to improve due to increase in transformation series. The single stage topology has a simple topology with high reliability and efficiency because of high power consumption, but control algorithm is more complex because of its power convert main circuit a new strategy is being developed. This paper describes a method for maximum power point tracking (MPPT) in the single-stage and three single-phase PV grid-connected system. In the paper, the nonlinear output characteristics of the PV including I-V & P-V are obtained in changed solar insulations or temperature based on MATLAB, and the MPPT algorithm which is

based on the P & O algorithm method, compared with Incremental Conductance, is also described, a dimensioning of the impedance adapter for better stabilization. A comparison SPWM and SVPWM control methods in the case of a grid connection applied to the electrical grid of Republic of Congo and their influences on the dynamic performance of the system and their impact in reducing the harmonic rate for better injection into the grid. The simulation model of three single-phase PV grid-connected system is built, and simulation results show the MPPT algorithm has excellent dynamic and static performances, which verifies the Incremental Conductance is effective for MPPT in the single-stage and three single-phase PV grid-connected system.

Keywords

Photovoltaic Array, Congo, Maximum Power Point Tracking, Perturbation Observation, Incremental Conductance, Partial Shading Conditions, Performance Evaluation, State Flow

1. Introduction

This paper presents the background and the motivation of the analysis of Maximum Power Point Tracking (MPPT) adaptability continuing with a short overview of grid-connected PV system. Furthermore, in detail the aims of the project, continuing with a list of the main contributions and finishing with the outline of the proposed method. The need for a cleaner environment and continuous increase in energy needs makes decentralized renewable energy production more and more productive. This continuously increasing energy consumption overloads the distribution grids as well as the power stations, therefore having an impact negatively on power availability, security and quality [1]. In the last decade solar energy technologies have become less expensive and more efficient, which have made it to an attractive solution, being cleaner and more environmentally energy resource than traditional ones like fossil fuels, coal or nuclear.

Nevertheless, a PV system is still much more expensive than traditional ones, due to high manufacturing costs of PV panels, the energy that drives them. The light from the sun is free, available almost everywhere and will still be present for millions of years. One of the major advantages of PV technology is that it has no moving parts. Therefore, the hardware is very robust; it has a long lifetime and low maintenance requirements. And, most importantly, it is one solution that offers environmentally power generation [2]. Nowadays PV panel are not used in space application but they are present in everyday life: powering wrist watches, small calculators, supplying loads in remote sites and, last but not least, they are connected to the grid, generating the green power of the future [3] Photovoltaic (PV) energy generation provides several advantages such as harmless to the environment and renewable. Furthermore, grid-connected PV energy generation represents a renewable energy growing alternative that's becoming more competitive [4]. Based on their implementation, complexity, flexibility, reliability and cost, the

MPPT methods can be evaluated on the basis of the speed and accuracy of generating maximum power point tracking and the proposed method. The disadvantage with multi-stage systems is that they have a relatively higher efficiency, large size and higher cost. The single stage has numerous advantages such as simple topology, low cost and high efficiency [5] [6]. Nevertheless, the control strategy has to be designed in order to extract the maximum available power and to properly transfer it from the PV array to the grid simultaneously. In this case a most important consideration in the controller design is needed. The performance evaluation of MPPT schemes is imperative because of their sensitive to various dynamics [7]-[23]. This study presents a major innovation as it is the first to be applied to the specific case of the analysis of MPPT adaptability in inverters of the three-phase photovoltaic systems integrated into the electrical grid of Congo-Brazzaville. This paper is organized as follows. Section 2 presents system description and modeling of PV array system. Section 2.1 presents the dynamic parameters of the whole system and modeling of solar cell and PV array model. Section 2.2 presents photovoltaic characteristics and grid-connected inverter models. Section 2.3 compares the dynamic parameters of incremental conductance (INC) algorithms and the dynamic parameters of Perturbation and observation(P&O) algorithms. Section 3 presents the whole simulation's results. Section 3.1 presents perturbation and observation (P&O) techniques. Section 3.2 presents incremental conductance (INC) techniques. Section 3.3 presents others MPPT schemes. Section 3.3 discusses the standard evaluating parameters partial shading conditions under different power and current. Section 3.4 presents accuracy by comparing, one of than better of their big size, high cost, low efficiency and high reliability. Therefore, in three phase single-stage grid connected PV system must achieve MPPT. Therefore, in order to generate the MPPT stability under irradiation and Temperature, a robust MPPT controller has been proposed. Section .4 concludes this article

2. Model of a Photovoltaic Cell

In the present modeling, the focus is only on cells. Solar cells consist of a p-n junction. The simplest equivalent circuit of a solar cell is a current source in parallel with a diode. The diode determines the I-V characteristics of the cell. For this paper, the electrically equivalent circuit of a solar cell is shown in **Figure 1** [2].

$$\begin{aligned}
 I &= I_{ph} - I_d - I_{sh} = I_{ph} - I_{do} - \frac{V + IR_s}{R_{sh}} \\
 &= I_{ph} - I_o \left\{ \exp \left[\frac{q(V + IR_s)}{AkT} \right] - 1 \right\} - \frac{V + IR_s}{R_{sh}}
 \end{aligned} \tag{1}$$

$$I_o = I_{do} \left(\frac{T}{T_{ref}} \right)^3 \exp \left[\frac{qE_g}{nk} \left(\frac{1}{T_{ref}} - \frac{1}{T} \right) \right] \tag{2}$$

$$I_{ph} = I_{sh} \left(\frac{S}{1000} \right) + C_T (T - T_{ref}) \tag{3}$$

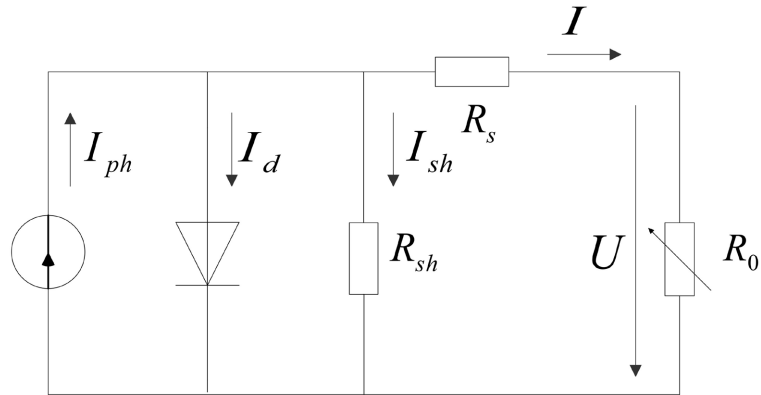


Figure 1. Solar cell electrically equivalent.

$$\begin{aligned}
 I &= I_{ph} - I_d = I_{ph} - I_o \left\{ \exp \left[\frac{q(V + IR_s)}{AkT} \right] - 1 \right\} \\
 &\approx I_{ph} - I_o \left\{ \exp \left[\frac{qV}{AkT} \right] - 1 \right\}
 \end{aligned}
 \tag{4}$$

When $I = 0$ in formula (4), the open circuit voltage can be deduced as:

$$V_{oc} = \frac{nkT}{q} \ln \left(\frac{I_{ph}}{I_o} + 1 \right)
 \tag{5}$$

Here, I_{ph} is the photocurrent, I_o is the reverse saturation current, I_{do} is the average current through the diode, n is the diode factor, q is the electron charge ($q = 1.6 \times 10^{-19}$), k is the Boltzmann's constant ($k = 1.38 \times 10^{-23}$ J/K), and T is the solar array panel temperature. R_s is the intrinsic series resistance of the solar cell; this value is normally very small, R_{sh} is the equivalent shunt resistance of the solar array, and its value is very large.

I_{sc} is photovoltaic battery short-circuit current; S is light intensity; C_T is the temperature coefficient; T is temperature of cell in Kelvin (K); T_{ref} is the reference temperature (298 K); E_g is the characterization of the width of the forbidden band semiconductor constants (V). In general, the output current of a solar cell is expressed by: Physical models based on physical mechanisms and mathematical models based on external characteristic. The model parameter setting based on external characteristic is more realistic. The photovoltaic array is modeled as follows [3] [4].

Under the conditions of any solar radiation intensity R ($\text{w}\cdot\text{m}^{-2}$) and ambient temperature T_a ($^{\circ}\text{C}$), the Photovoltaic array temperature T_c ($^{\circ}\text{C}$) is:

$$T_c = T_a + t_c \cdot R
 \tag{6}$$

In the formula, R is the light radiation of the Photovoltaic array and t_c ($\text{w}^{-1}\cdot\text{m}^2$).

In the formula, R is the light radiation of the Photovoltaic array and t_c ($\text{w}^{-1}\cdot\text{m}^2$) is the temperature coefficient of the photovoltaic array. Under the reference, I_{sc} is the short-circuit current, V_{oc} is the open-circuit voltage, and I_m , V_m is the current and voltage at the maximum power point, then when the photovoltaic

array voltage is V , its current is I the following equation represents the equivalence of short circuit current and temperature coefficient, fundamental to relativity:

$$I = I_{sc} \left(1 - C_1 \left(e^{\frac{V}{C_2 V_{oc}}} - 1 \right) \right) \quad (7)$$

where C_1 represents the dynamic of parameter temperature coefficient, as follows as:

$$C_1 = (1 - I_m / I_{sc}) e^{-\frac{V_m}{C_2 V_{oc}}} \quad (8)$$

where C_2 represents also the dynamic of parameter temperature coefficient, as follows as:

$$C_2 = (V_m / V_{oc} - 1) / \ln(1 - I_m / I_{sc}) \quad (9)$$

In the current research considering solar irradiation and temperature changes

$$I = I_{sc} \left(1 - C_1 \left(e^{\frac{V}{C_2 V_{oc}}} - 1 \right) \right) + DI \quad (10)$$

where DI are the variation of current of solar and photovoltaic array, as follows as:

$$DI = \alpha \cdot R / R_{ref} \cdot DT + (R / R_{ref} - 1) \cdot I_{sc} \quad (11)$$

where DV are the variation of voltage of solar and photovoltaic array, as follows as:

$$DV = -\beta \cdot DT - R_s \cdot DI \quad (12)$$

where DT are the variation of temperature of solar and photovoltaic array, as follows as:

$$DT = T_c - T_{ref} \quad (13)$$

where R_{ref} , T_{ref} are the reference values of solar radiation and photovoltaic array temperature, generally 1 kW/m^2 , 25°C ;

Where α represents: Under the reference sunshine, the temperature coefficient of current change (Amps/ $^\circ\text{C}$);

Where β represents: Under the reference sunshine, the temperature coefficient of voltage change (V/ $^\circ\text{C}$);

Where R_s represents: The series resistance of the Photovoltaic array.

An important parameter for evaluating the performance of photovoltaic cell is the fill factor (FF) which is [5]:

$$FF = \frac{U_m I_m}{U_{oc} I_{sc}} \quad (14)$$

The molecule in formula (15) is P_m and the fill factor reflects the conversion efficiency of the photovoltaic array to a certain extent. The maximum conversion

efficiency that a photovoltaic can obtain is [5]:

$$\eta_m = \frac{P_m}{P_{in}} \tag{15}$$

2.1. Photovoltaic Characteristic and Grid Connected Inverter Model

According to the characteristics of solar energy photovoltaic battery monomer equation according to of certain rules of series and parallel form photovoltaic array change different intensity of illumination and temperature, we can draw as **Figure 2** and **Figure 3** showed of photovoltaic array nonlinear output characteristic curve is:

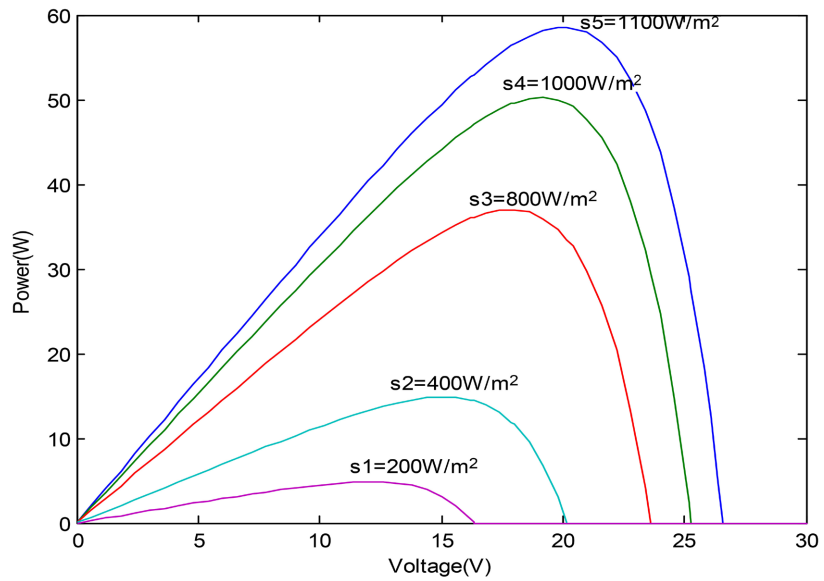


Figure 2. PV cell characteristic curves under different illuminations ($T = 273 \text{ K}$).

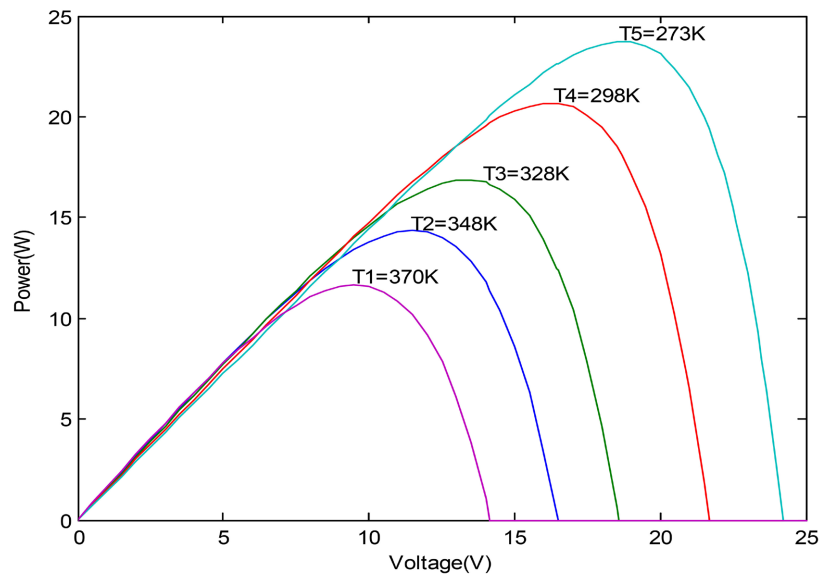


Figure 3. PV cell characteristic curves under different temperature ($S = 500 \text{ W/m}^2$).

Topology diagram of a three-phase photovoltaic system connected to an inverter. In **Figure 4**:

- PV represents the photovoltaic panel.
- C is the DC bus capacitor.
- T1 to T6 are the six IGBTs of the three-phase inverter bridge [6] [7].

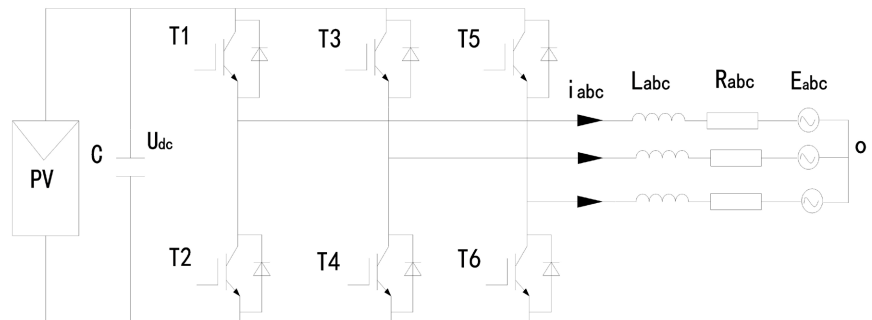


Figure 4. Three phase photovoltaic grid-connected inverter model.

In the three-phase stationary coordinate system, according to Kirchhoff's current and voltage laws, the current and voltage equations of the grid-connected inverter can be obtained as [7]:

$$C_1 \frac{du_{dc}}{dt} = i_{pv} - \sum_k i_k s_k \tag{16}$$

$$L \frac{di_k}{dt} + Ri_k = u_{kn} - u_{sk} - u_{on} \tag{17}$$

$$u_{kn} = u_{dc} \cdot s_k \tag{18}$$

$$u_{kn} = u_{ko} + u_{on} \tag{19}$$

$$\sum_k i_k = \sum_k u_{sk} = 0 \tag{20}$$

Because the load of the photovoltaic inverter is symmetrical, the neutral point is 0. According to Equations (16) (20) it can be obtained:

$$u_{on} = \frac{u_{dc}}{3} \cdot \sum_k s_k \tag{21}$$

$$\sum_k u_{ko} = \sum_k u_{kn} - 3u_{on} = 0 \tag{22}$$

where $k = a, b, c$ represents the switching state of an inverter bridge: When $s_k = 1$ indicates the upper arm of the PV inverter is on and the lower arm is off, and $s_k = 0$ indicates the upper arm is off and the lower arm is on. The inverter model in the three-phase stationary coordinate system is straightforward, but time-varying grid components complicate controller design. To simplify, this paper transforms the model from the three-phase stationary system to the synchronous rotating (d-q) system with the grid frequency. This conversion changes AC components to DC, easing control design.

First, Clarke transformation converts the three-phase system to a two-phase

stationary system, aligned with phase A of the grid [8]. The mathematical model of the photovoltaic inverter synchronous coordinates, as shown in **Figure 5**.

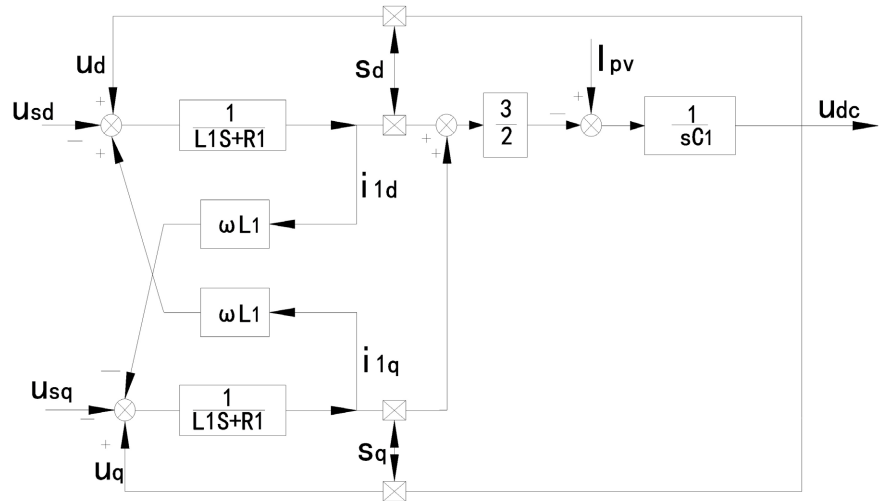


Figure 5. Mathematical model of the photovoltaic inverter under synchronous coordinates.

When the grid voltage is constant and inverter losses are neglected, the DC voltage of the grid-connected inverter is proportional to the d-axis component of the output current, and the active power p is also proportional to this current. Thus, the DC voltage can be controlled by regulating the active power [9].

Figure 6 shows that the grid-connected inverter control system has an outer DC voltage loop and an inner loop for active and reactive currents. The DC voltage loop stabilizes or adjusts the DC side voltage. Due to the single-stage topology, the system often faces energy accumulation and DC voltage variations, which can lead to system collapse. DC voltage feedback can be achieved without static control using a PI controller.

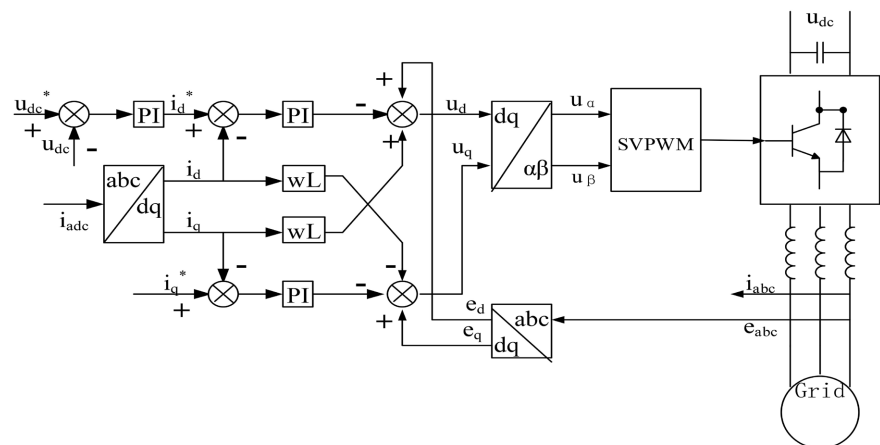


Figure 6. Grid-connected inverter control block diagram based on grid voltage orientation.

The design of the voltage loop primarily aims to enhance the power supply's

ability to withstand interference with the load and is designed according to a type II system. To reduce overshoot, a filter link can be added to the reference voltage, or a ramp setting can be used to make the reference voltage change gradually. Assuming that the three-phase currents are symmetrical, the instantaneous power on the three-phase AC inductor is zero. We establish:

$$C_1 \frac{du_{dc}}{dt} \cdot u_{dc} = u_{dc} i_{pv} - \frac{3}{2} e_d i_d \quad (23)$$

It is further transformed to:

$$C_1 \frac{du_{dc}}{dt} = i_{pv} - \frac{3e_d}{2u_{dc}} i_d \quad (24)$$

Since the values of e_d and u_{dc} do not change much $-3e_d/2u_{dc}$, it can be represented by the constant K . Without considering the DC side disturbance, the transfer functions of active current and Dc voltage are expressed as

$$\frac{U_{dc}(s)}{I_d(s)} = \frac{K}{sC_1} \quad (25)$$

Let the PI regulator control equation be:

$$i_q^* = \left(K_p + \frac{K_i}{s} \right) (u_{dc}^* - u_{dc}) = K_p \left(\frac{\tau s + 1}{\tau s} \right) (u_{dc}^* - u_{dc}) \quad (26)$$

Knowing the current closed-loop transfer function, $w(s) = 1/(3T_s s + 1)$ and considering the DC voltage sampling delay (e^{-T_s}), it can be approximated as $1/(Ts + 1) = 1/(4T_s + 1)$. Combine equations (35) and (36) to get the voltage open-loop transfer function

$$\omega_o(s) = \frac{K_p K (\tau s + 1)}{C_1 \tau s^2 (Ts + 1)} \quad (27)$$

According to a typical type II system design there are:

$$\frac{K_p K}{C_1 \tau} = \frac{h + 1}{2\tau^2} \quad (28)$$

Taking the intermediate bandwidth, $h = \frac{\tau}{4T_s} = 5$, we get:

$$K_p = \frac{3C_1}{20KT_s} \quad (29)$$

$$K_i = \frac{K_p}{20T_s} \quad (30)$$

Design of the current loop PI, the sampling period of the current loop is the PWM switching period, T_s the data acquisition $e^{-T_s s}$ and $e^{-0.5T_s s}$ control delays are respectively, the delay link can be equivalent to $1/(1.5T_s s + 1)$.

The d and q-axis current control is symmetrical control, so taking the d-axis as an example, S-domain model of the PI controller is:

$$k_p + \frac{k_i}{s} = \frac{k_p(\tau_i s + 1)}{\tau_i s} \tag{31}$$

According to the typical $\tau_i = L/R$, **Figure 5** as shown of the PI controller is

$$W_o(s) = \frac{k_p}{R\tau_i s(1.5T_s s + 1)} \tag{32}$$

Then the PI controller parameters can be obtained:

$$k_p = \frac{R\tau_i}{3T_s} = \frac{L}{3T_s} \tag{33}$$

$$k_i = \frac{k_p}{\tau_i} \tag{34}$$

where k_p and k_i are the proportion coefficient and integral coefficient, respectively.

In this paper, we connected the photovoltaic system-inverter to the electricity grid of the Republic of Congo. The schematic representation of the electricity transmission network, shown in a single-line diagram (see **Figure 7**), provides a detailed overview of the elements of this complex network. This representation is crucial for understanding the layout and operation of the components that ensure electricity distribution across the country.

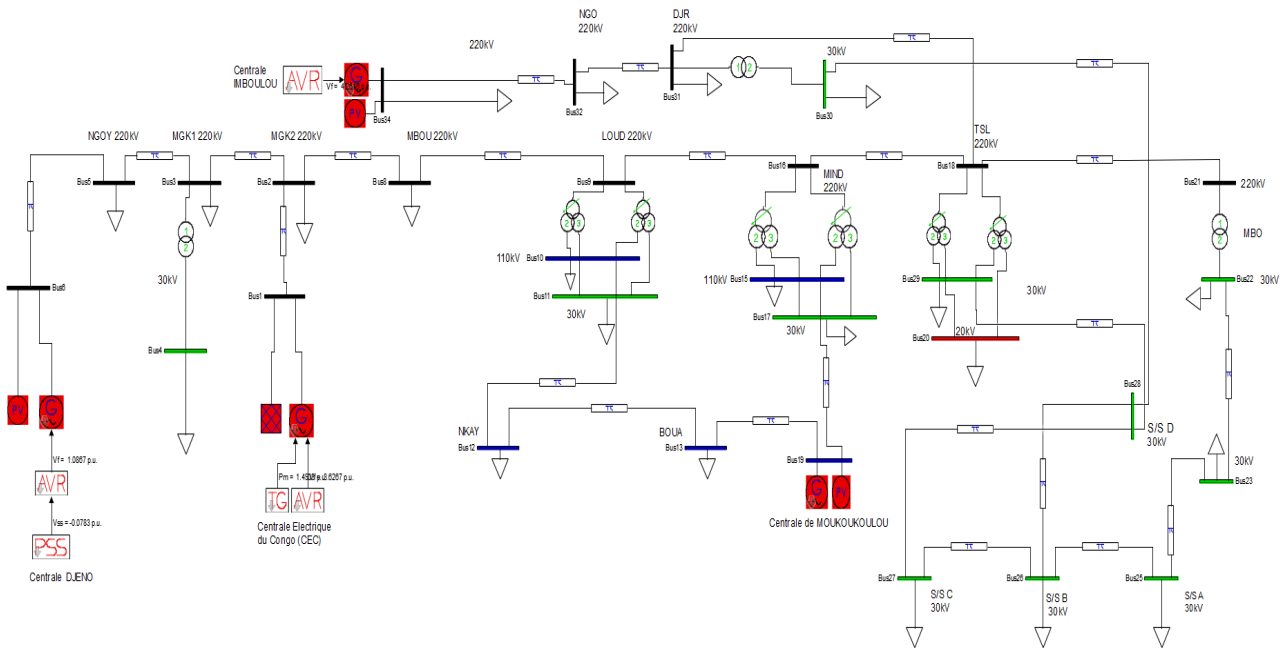


Figure 7. Power transmission network of the Republic of Congo.

Firstly, the network consists of five power generation plants: The Congo Electric Power Plant (CEC) at node (1) located in the Pointe-Noire department, the Imboulou Power Plant at node (34) situated in the Pool department, the Djeno Power Plant at node (6) in the Pointe-Noire department, the Moukougoulou Power Plant at node (19) in the Bouenza department, and finally, the Djoué Power

Plant at node (23) in the Pool department, which is currently out of service. These plants play a crucial role in generating the energy necessary to supply the country. They are strategically located at various points across the Congolese territory to meet energy needs in a balanced manner. The geographical distribution of these plants aims to optimize production and minimize line losses.

Regarding consumption, the network includes 22 loads, representing the various locations where electricity is used. These loads are primarily localities situated across different departments throughout the network. Effective management of these loads is essential to ensure a stable and reliable supply to end users.

The network also features 24 transmission lines, which transport the electricity produced by the power plants to the loads. These lines often cover long distances, requiring rigorous planning and careful management to maintain distribution reliability. The transmission line infrastructure must be meticulously designed to minimize interruptions and ensure continuous delivery of electricity.

Finally, the network comprises 34 nodes, which are convergence points for the transmission lines. These nodes play a strategic role in the network by allowing the redistribution of electricity in various directions. Through these nodes, the network can be organized in a meshed manner, significantly improving supply security. In the event of a failure or malfunction in part of the network, the nodes enable the redirection of electricity through alternative routes, thereby ensuring service continuity.

The geographic and schematic representation of the electricity transmission network of the Republic of Congo offers a detailed and precise view of the entire system. It clearly visualizes the arrangement of power plants, loads, transmission lines, and nodes. This comprehensive view is essential for effective network management, facilitating its maintenance and future improvements

2.2. Principle of MPPT Control Based on the Perturb and Observe (P&O) Algorithm

P&O is an advanced control technology for maximum power point tracking MPPT [10] [11] [12] [22].

We design an intelligent algorithm to generate a reference voltage for the DC link. To overcome the limitations of the traditional P&O method, we have adopted a variable step size method, integrated into the MPPT control of a single-stage three-phase photovoltaic system. Simulations show improved performance [10] [11] [16] [20]-[23] with this method. Based on the DC reference voltage, the DC-AC converter adjusts the operating cycle. The behavior of solar panel indicating MPP and operating principle is shown in **Figure 8** which indicates that the resulting change of PV power is observed as follows. When the PV module operating point is on the left side of the curve ($\frac{\Delta P}{\Delta V}$ is positive) which means the PV module output power increases, the perturbation of the PV module voltage should increase toward the MPP.

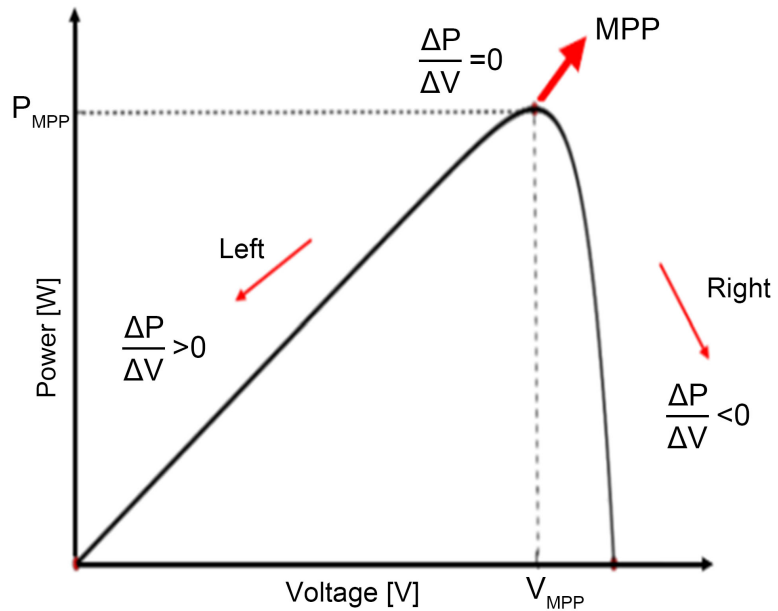


Figure 8. Behavior of solar panel indicating MPP and operating principle.

If the operating point of the module was on the right side of the curve $\frac{\Delta P}{\Delta V}$ is (negative), then the perturbation of the PV module voltage should be decreased toward the MPP.

A PI controller adjusts the DC voltage according to the measured error. This MPPT approach reacts more quickly to power variations caused by simultaneous changes in speed and irradiation, with irradiation estimated from the PI controller's error. The DC voltage controller sets the reference current for the current controller, aiming to maintain a constant DC voltage despite rapid changes in atmospheric conditions.

Performance evaluation techniques are discussed on the basis of the dynamic parameters of the PV system. By comparing between two algorithms which are incremental conductance and P&O algorithm; improved incremental conductance algorithms, perturbations and observations techniques, one of them is better than others [10]-[22]; the algorithm is the advanced control of technology one of the best, fastest and very easy to code. Due to the energy loss during the confusion and recovery periods when irradiance changes, direct duty ratio control offers better energy utilization and better stability characteristics with the proposed of methods which are P&O algorithm. From **Figures 8-10**, it can be seen that there is only one maximum power point under a certain light intensity, that is $\frac{dP}{dU} = 0$. Taking the derivation of the voltage U on both sides of the instantaneous output power of the photovoltaic cell, the basic equation of this algorithms are follows as:

$$P = U \cdot I \quad \text{then} \quad (35)$$

Taking the derivation of the voltage U on both sides of the instantaneous output power of the photovoltaic cell, $P = U \cdot I$ then is power of the cell since

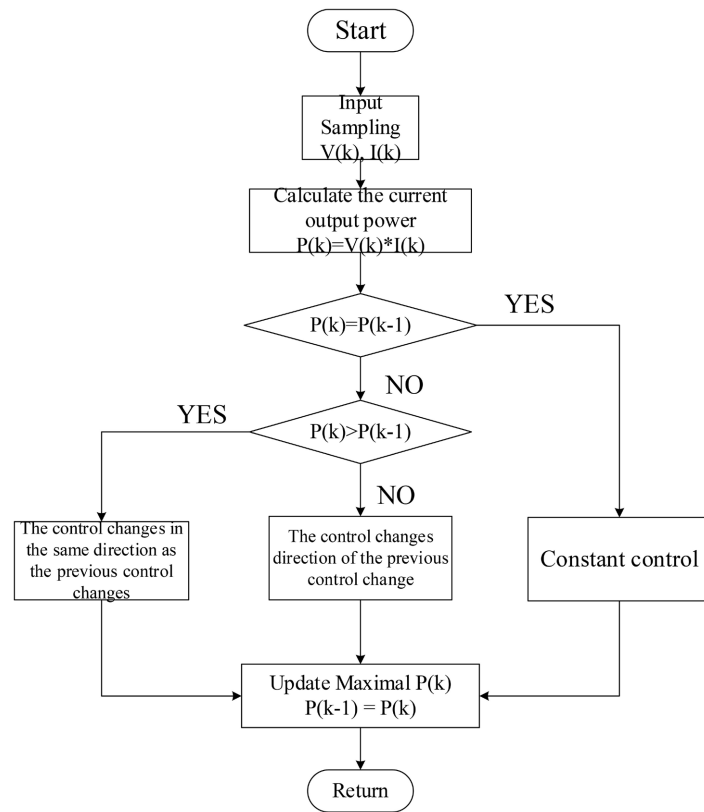


Figure 9. Flow chart of the P&O algorithm.

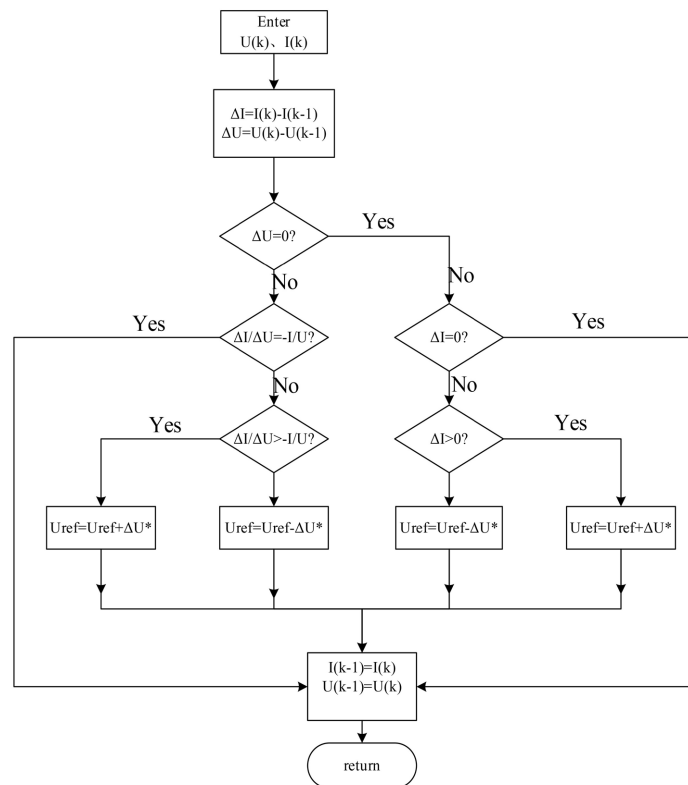


Figure 10. Flow chart of the incremental conductance algorithm.

$$\frac{dP}{dU} = I + U \frac{dI}{dU} \cong I + U \frac{\Delta I}{\Delta U} \quad (36)$$

Then $\frac{dP}{dU} = 0$, is the output power of the photovoltaic cell reaches the maximum. Then it can be deduced that the following relationship must be satisfied when the operating point is at the maximum power point:

$$\frac{dI}{dU} = -\frac{I}{U} \quad (37)$$

Where $\frac{\Delta I}{\Delta U}$ is then the variation of current as follows as: Approximately $\frac{dI}{dU}$ is replacing, the criterion for maximum power tracking using the incremental conductance method as follows:

$$\frac{\Delta I}{\Delta U} > -\frac{I}{U} \quad \text{Left side of MPPT} \quad (38)$$

$$\frac{\Delta I}{\Delta U} = -\frac{I}{U} \quad \text{At the MPPT} \quad (39)$$

$$\frac{\Delta I}{\Delta U} < -\frac{I}{U} \quad \text{right side of MPPT}, \quad (40)$$

The MPP can thus be tracked by comparing the instantaneous conductance $\frac{I}{U}$ to the incremental conductance $\frac{\Delta I}{\Delta U}$ and accordingly the voltage perturbation sign is determined still reaching the MPP [10] [11] [16]. The flow chart of the conventional Incremental conductance algorithm is shown in **Figure 10**. If the irradiance increases or decreases, that's, PV current increases or decreases, the MPP moves to right (left) with respect to PV voltage. When compared with this proposed method, low cost MPPT algorithms as P&O Algorithm [22], the main advantage of the incremental conductance algorithms is that it can determine the accurate direction to reach the MPP thus decreasing the steady-state oscillation and improving system response under rapidly changing conditions [10]-[22]. However, regarding the algorithm structure, conventional incremental conductance algorithm includes a number of division calculations and relatively complex decision-making process which in turn raises the need of a more powerful micro controller featuring higher clock frequency, larger memory and floating-point calculation capability decreasing the possibility of achieving a low cost. A solution to this conflicting situation is to have a variable step-size that gets smaller towards the MPP in order to balance the competing aims of convergence speed and tracking accuracy.

The scope $\frac{\Delta P}{\Delta U}$ can be calculated using the PV module voltage and current. The incremental conductance algorithm is derived by differentiating the PV module power with respect to voltage and setting the results equal to zero. For a direct control scheme which directly controls the converter switching without external control loops, the considered step is the change in converter duty ratio ΔD as shown in Equations (41)-(44).

$$\Delta D = N_1 \frac{\Delta P}{\Delta U} \tag{41}$$

$$\Delta P = P(k) - P(k-1) \tag{42}$$

$$\Delta U = U(k) - U(k-1) \tag{43}$$

$$\Delta D = D(k) - D(k-1) \tag{44}$$

And N_1 is the scaling factor tuned at the design stage to adjust the conventional step-size ΔD to compromise between tracking accuracy [10] [18] and its convergence speed. The flow chart of the incremental conductance method is shown in **Figure 10**. The main advantage of using the incremental conductance method [10] [11] is that the adaptability and control stability of the MPPT is high.

Stateflow is a MATLAB tool used to model and simulate decision logic systems and state machines, making it easier to design complex systems where states change based on events or conditions, as shown in **Figure 11**.

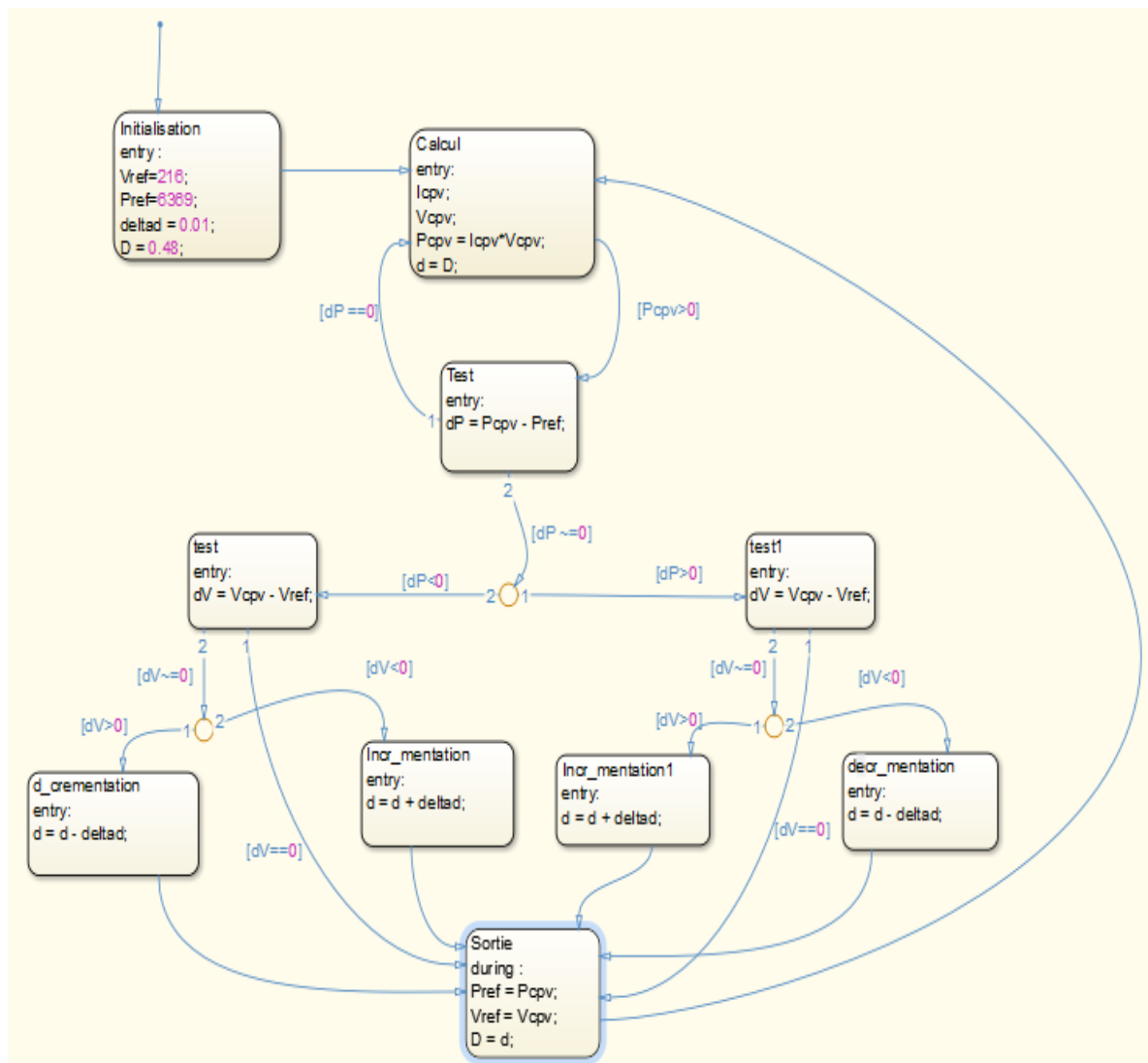
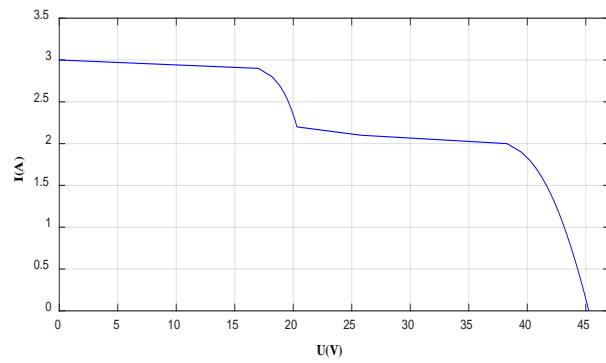
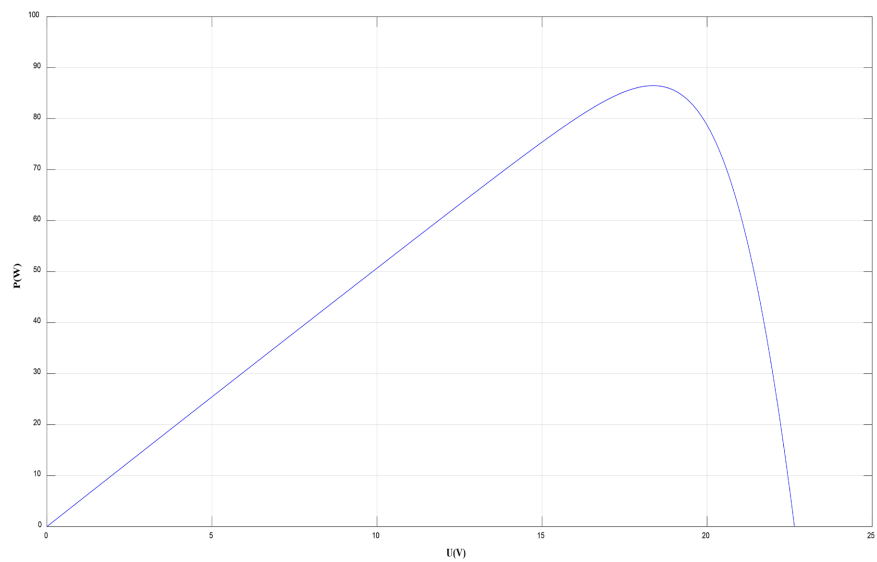


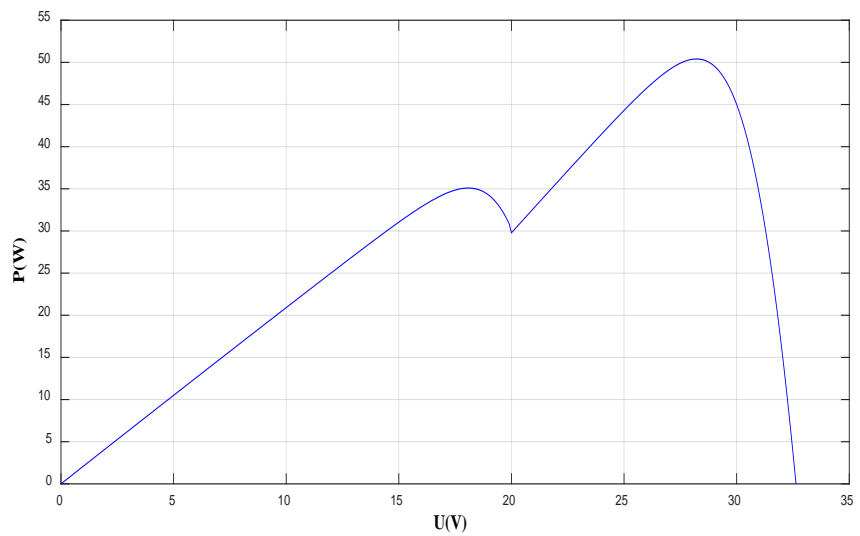
Figure 11. State flow of the of the incremental conductance algorithm.



(a) PV current characteristic under partial shading



(b) PV characteristics under uniform irradiance



(c) PV Power characteristic under partial shading

Figure 12. Assessment of Proposed Incremental Conductance MPPT Algorithm Partial Shading. (a) PV current characteristic under partial shading; (b) PV characteristics under uniform irradiance; (c) PV Power characteristic under partial shading.

Assessment of Proposed Incremental Conductance MPPT Algorithm Partial Shading, in conventional MPPT systems the energy produced by the shaded cell as complete power extraction from the PV array, can be preserved because it is inhibited by the cell [12] [23]. As shown in **Figure 12** and also PV the characteristic of under uniform irradiance.

3. Simulation Results

In this section, we will first present the time evolution of output power, output voltage, current, and Harmonic Distortion Rate using the MPPT algorithm based on the P&O method [22]. Next, we will show the results for these same output parameters using the MPPT algorithm based on the Conductance Increment method [10] [11] [16]-[21] and [23].

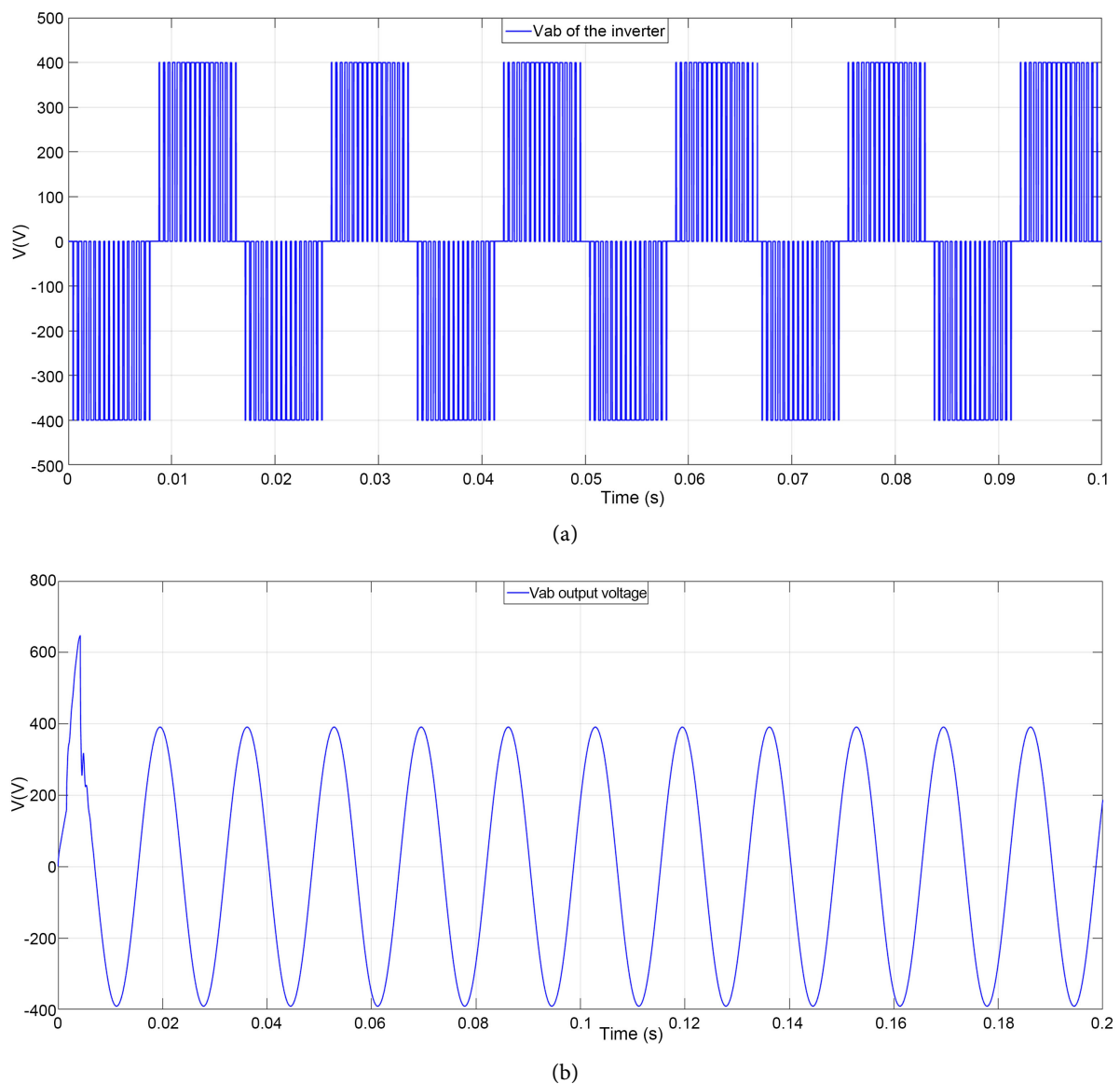


Figure 13. (a) Voltage of the inverter and (b) output voltage.

- Voltage of the inverter

Figure 13 shows the graph of the output voltage of the DC/AC converter with pulse-width modulation. This graph illustrates the performance in terms of voltage of the inverter.

It can be observed from **Figure 13** that the voltage of an inverter must be stable, well-regulated, and as close as possible to a pure sinusoid to ensure efficient and safe operation of electrical equipment and compatibility with electrical grids.

- Output current

In this section, **Figure 14** shows the electrical current that the inverter supplies to the electrical grid after converting direct current (DC) into alternating current (AC).

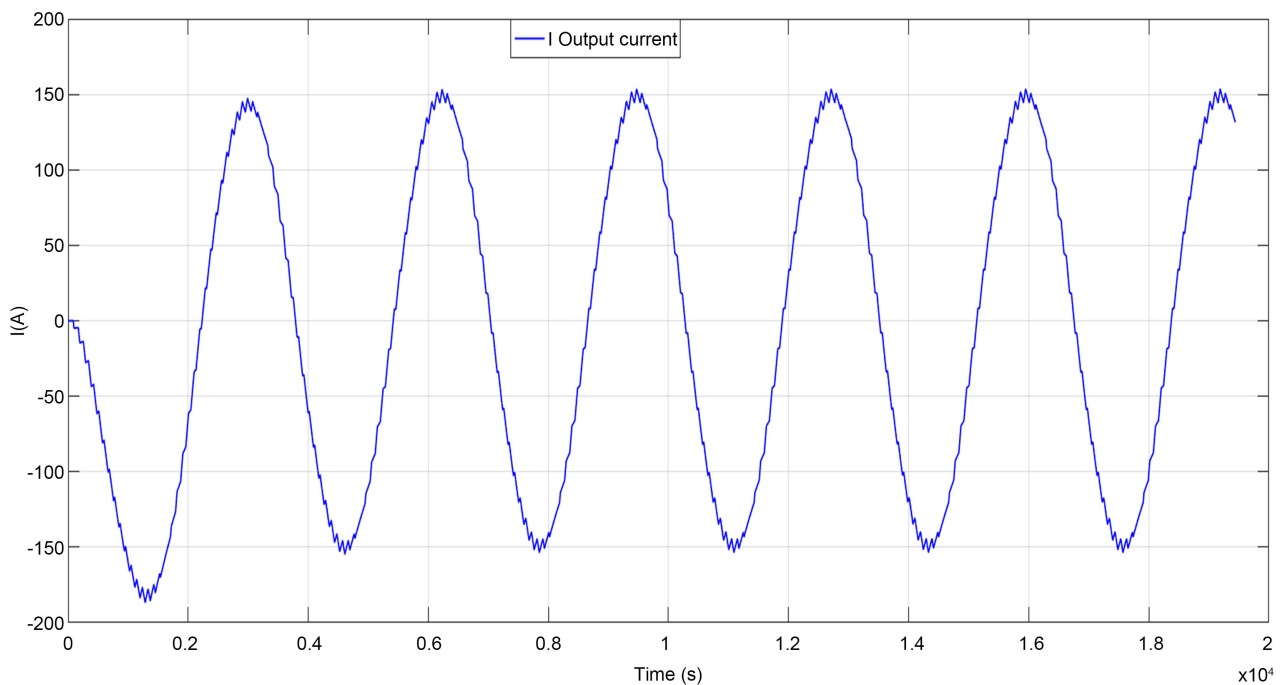


Figure 14. Output current.

It can be observed in **Figure 15**, that, although the current injected into the electrical grid by a PWM-controlled inverter is designed to be sinusoidal, it may contain harmonic components due to the modulation techniques.

- Power of the inverter

The PWM waveform of the power produced by the inverter contains harmonics, as shown in **Figure 15**, which are multiples of the fundamental frequency. These harmonics can be reduced by filters to improve the quality of the AC waveform and, consequently, the active power. **Figure 16** illustrates the harmonic distortion rate.

- Harmonic distortion rate

The total harmonic distortion (THD) is an important parameter when discussing the performance of an inverter. It measures the quality of the alternating

current (AC) produced by the inverter and is expressed as a percentage. **Figure 16** shows the total harmonic distortion of the inverter.

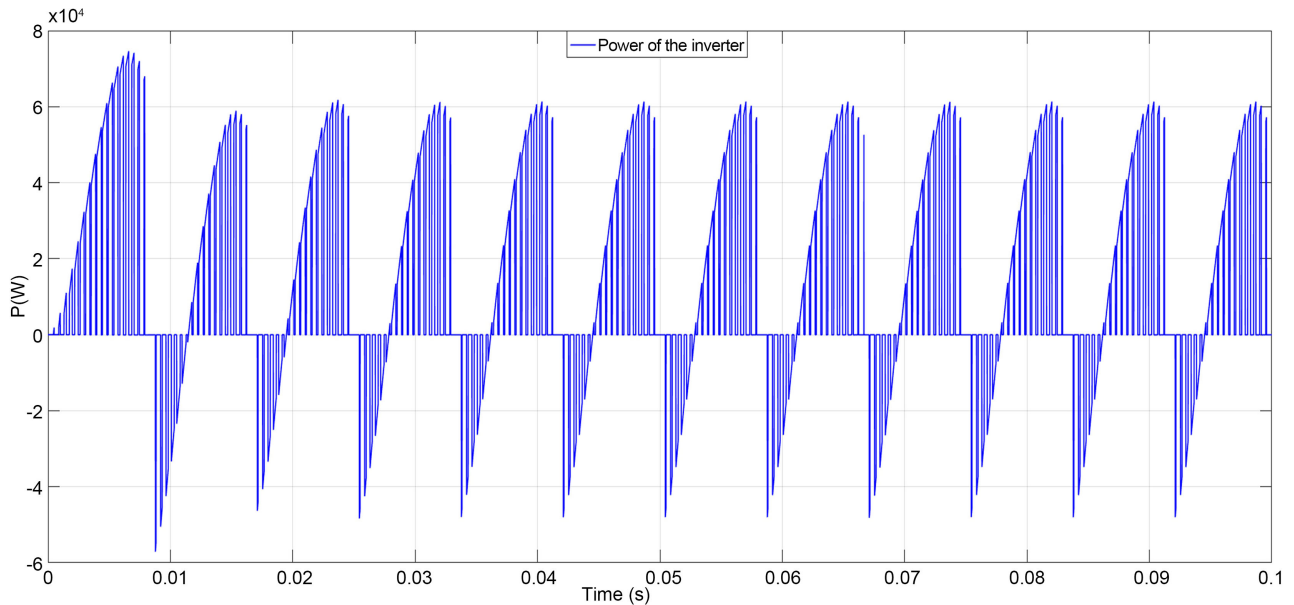


Figure 15. Power of the inverter.

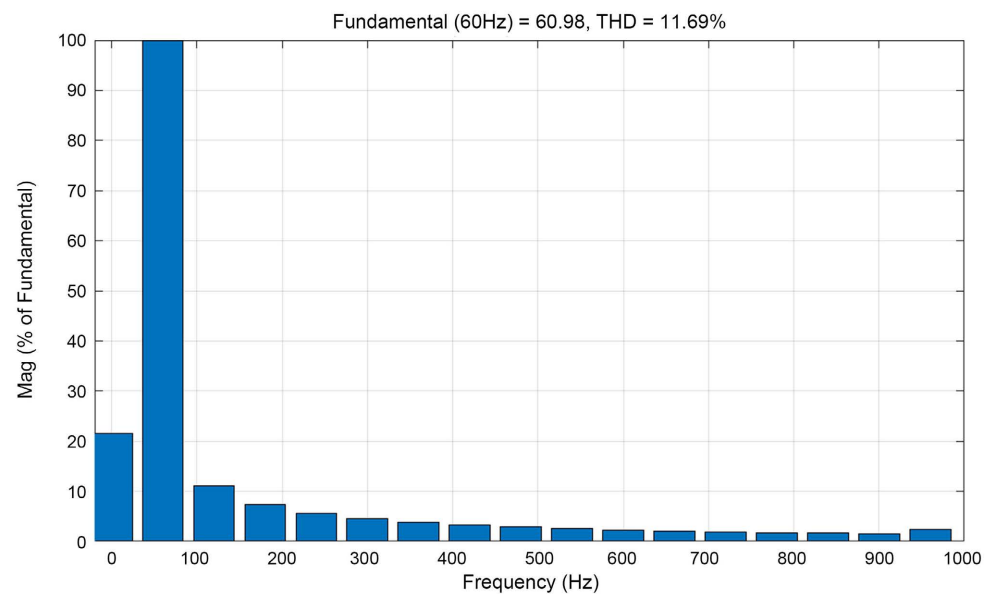
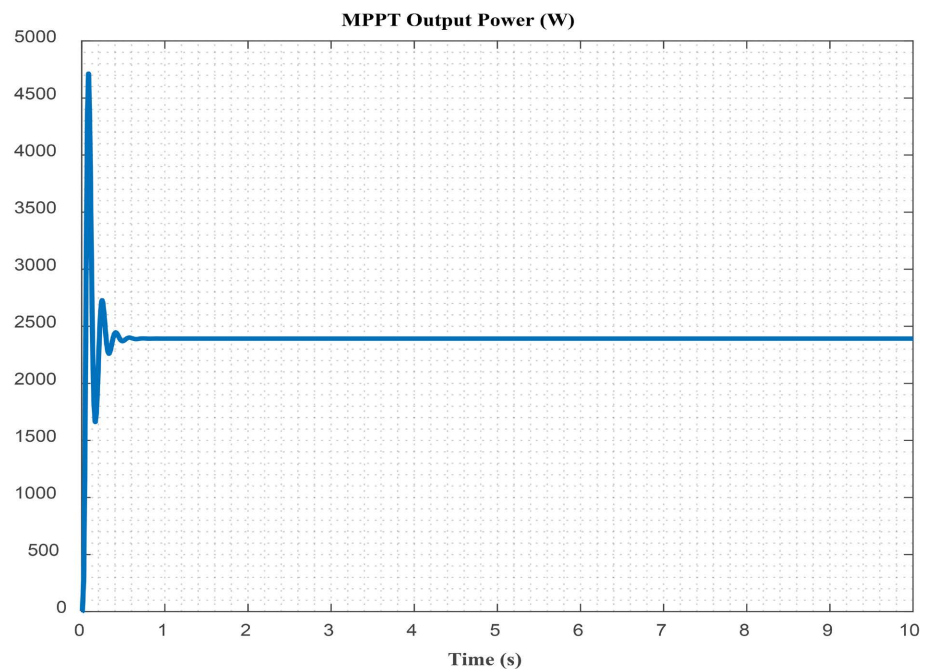


Figure 16. Harmonic distortion rate.

- **MPPT output power**
- Commonly used maximum power tracking control algorithms include constant voltage tracking algorithm (CVT), interference observation method (P&O), incremental conductivity method (IC), etc.
- The CVT method has the advantages of simple control, high reliability, and good stability, and is much more advantageous than direct coupling without CVT.

- However, this tracking method ignores the influence of temperature on the open-circuit voltage of the PV array, and the CVT method cannot completely track the maximum power point of the PV array in all temperature environments, and the system will oscillate.
- The P&O method is simple to control, which is more convenient to realize and improves the utilization efficiency of the system.
- However, its disadvantage is that in the steady state, it can only oscillate near the maximum power point, resulting in a certain power loss, and the setting of the tracking step can not take into account the tracking accuracy and response speed, and the algorithm itself is not rigorous, and the tracking error occurs when the sunshine intensity changes.
- Theoretically, the Incremental Conductance method [10] [11] [18] is better than the interference observation method, because the direction of change in the next moment depends entirely on the relationship between the rate of change of conductance and the instantaneous negative conductance value at that moment, so it can adapt to the rapid change of sunshine intensity, and its control effect is good, and it is not affected by the power time curve, but because the values of dI and dU are very small, it is relatively difficult to achieve, and there is still jitter under the condition of strong changes in external temperature.
- Due to the nonlinear characteristics of photovoltaic power generation system, the proposed of methods are used to solve the problem of maximum power point tracking (MPPT), which can make up for the shortcomings of some traditional control methods, such as the sensitivity of control parameters, the limitation of the scope of application, etc. **Figure 17** below shows the active power, voltage, and output current obtained using the P&O algorithm.



(a)

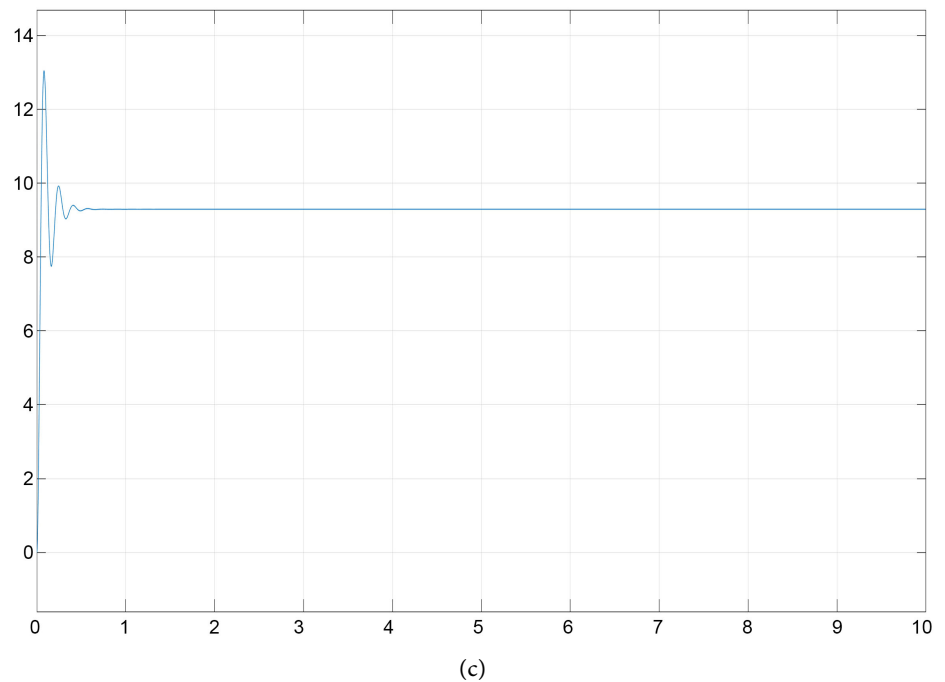
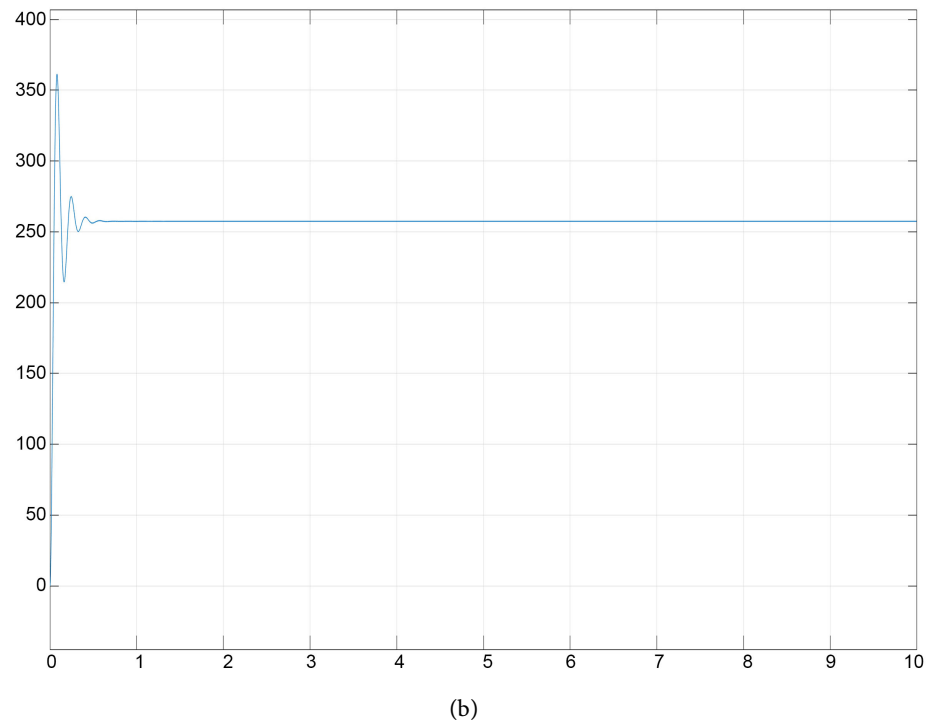


Figure 17. (a) MPPT Power of the P&O Algorithm, (b) MPPT Voltage of the P&O Algorithm and (c) MPPT Current of the P&O Algorithm.

The conductance method, as shown in **Figure 18**, allows for more precise and faster tracking of the maximum power point.

- **Luminous radiation power**

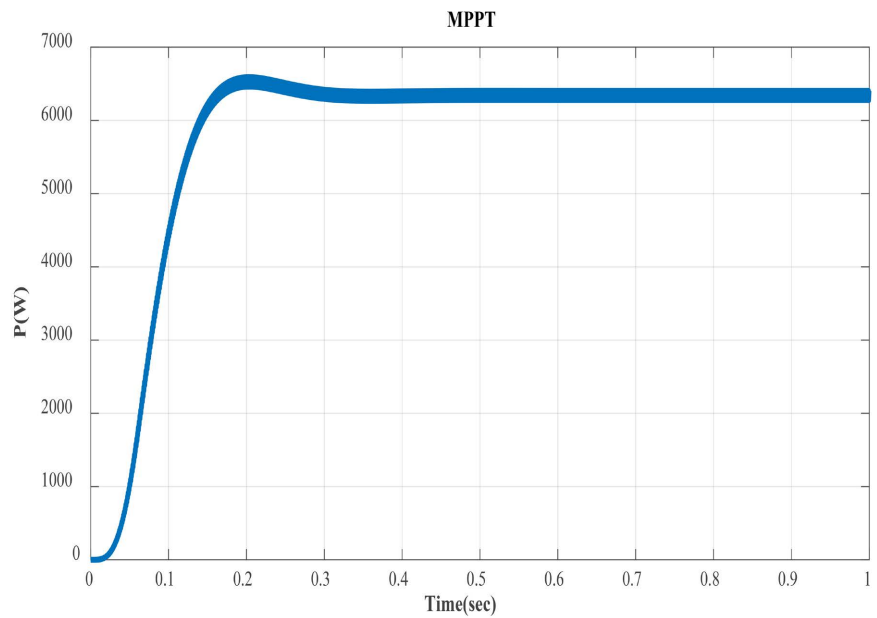
Irradiance is a measure of the power of luminous radiation received per unit area. In other words, it is the amount of light energy falling on a given surface per

unit of time. **Figure 20.** shows the evolution of luminous radiation power per unit area [12] [23].

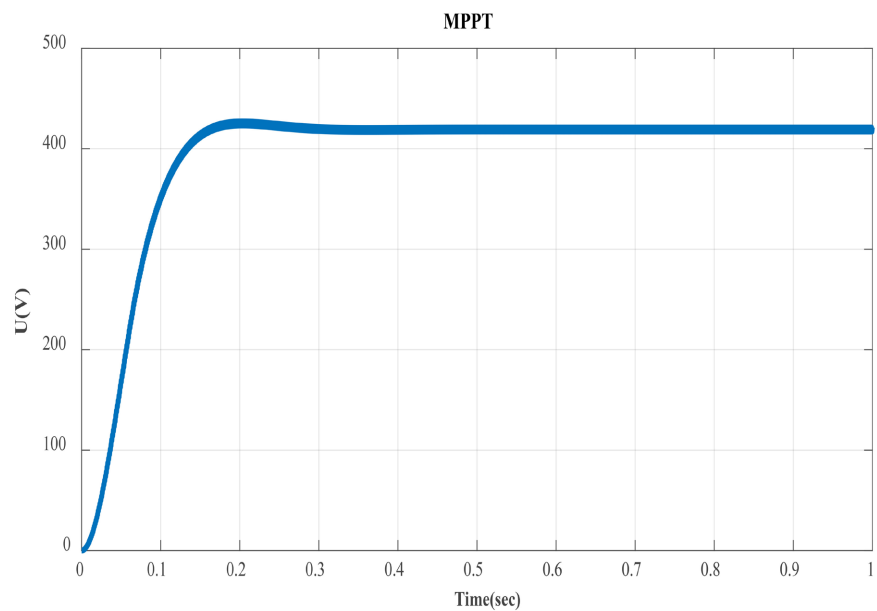
It is observed from **Figure 19.** that the luminous radiation power is approximately 220 W for an irradiance of 500 W/m², which corresponds to a surface area of 0.4 m². It is also noted that this radiation power decreases proportionally with the irradiance.

- **Current variation with irradiated area**

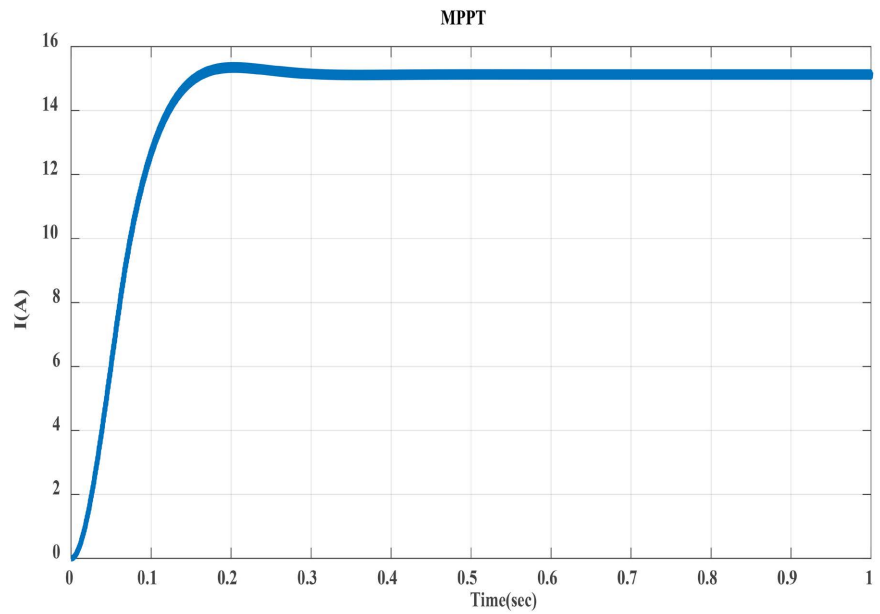
An increase in irradiance results in an increase in current for all voltage values, as illustrated in **Figure 20** below.



(a)



(b)



(c)

Figure 18. (a) MPPT power of the incremental conductance algorithm, (b) MPPT Voltage of the incremental conductance algorithm and (c) MPPT current of the incremental conductance.

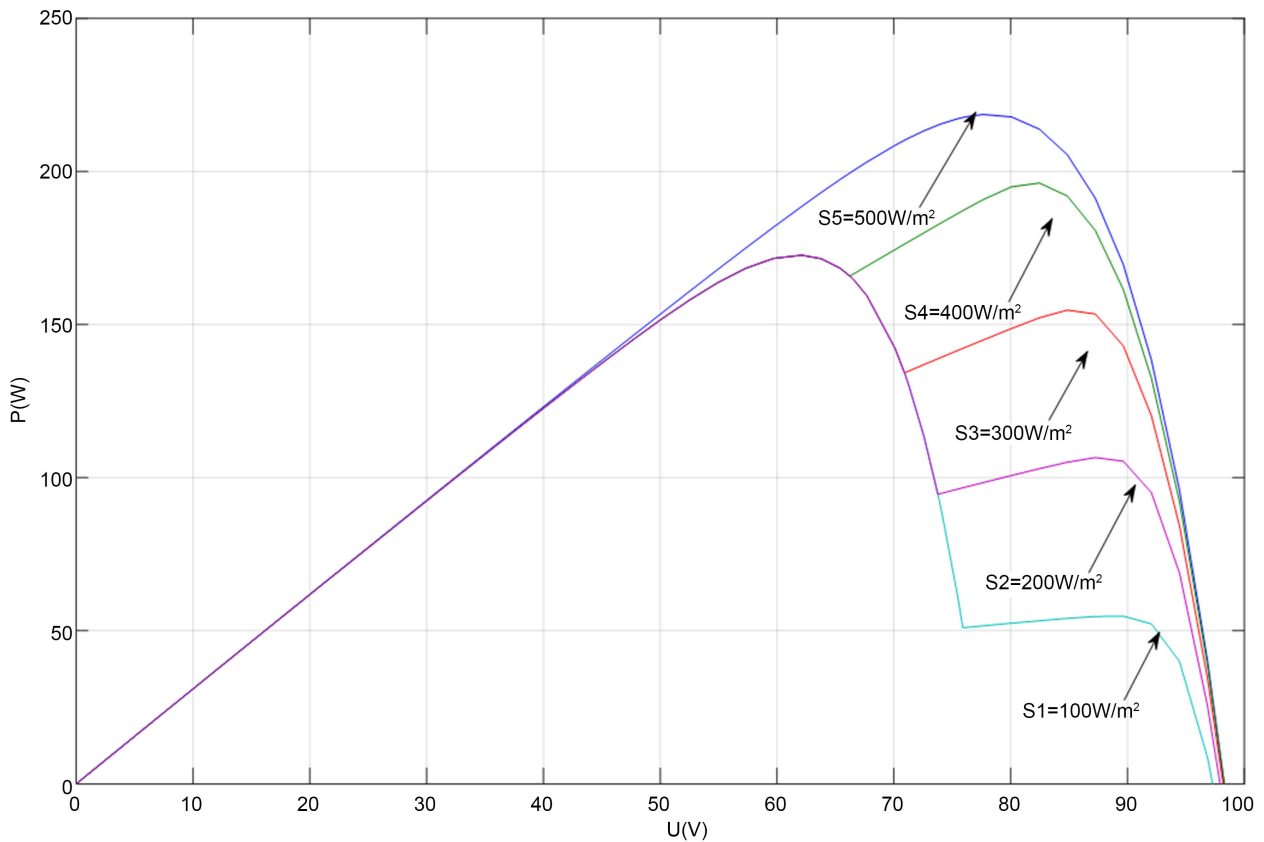


Figure 19. Partial shading conditions under different luminous radiation power.

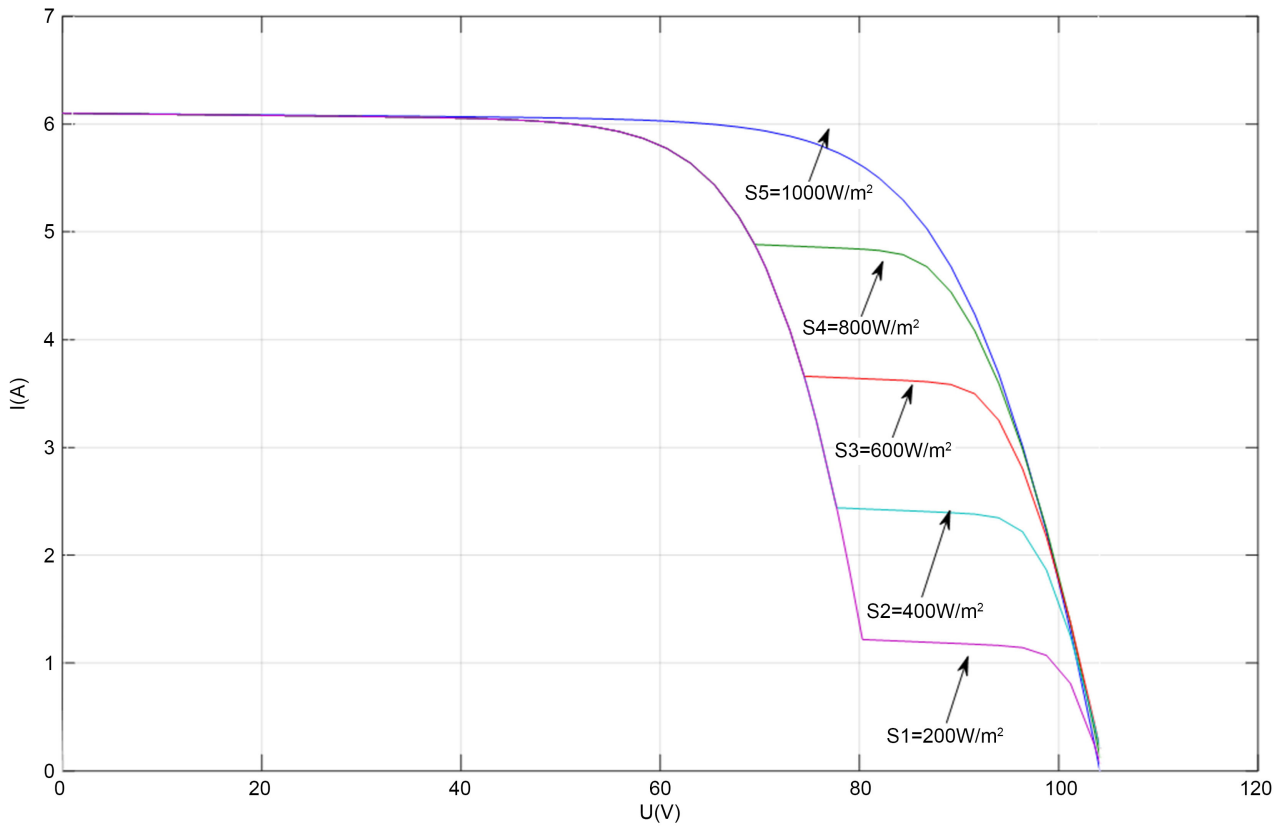


Figure 20. Partial shading conditions under different current variation with irradiated area.

It is observed that when the irradiated area of a photovoltaic panel decreases, the total number of photons captured by the panel also decreases. This reduction in the number of photons received leads to a decrease in the current produced by the panel. **Figure 21.** shows the variation of the duty cycle.

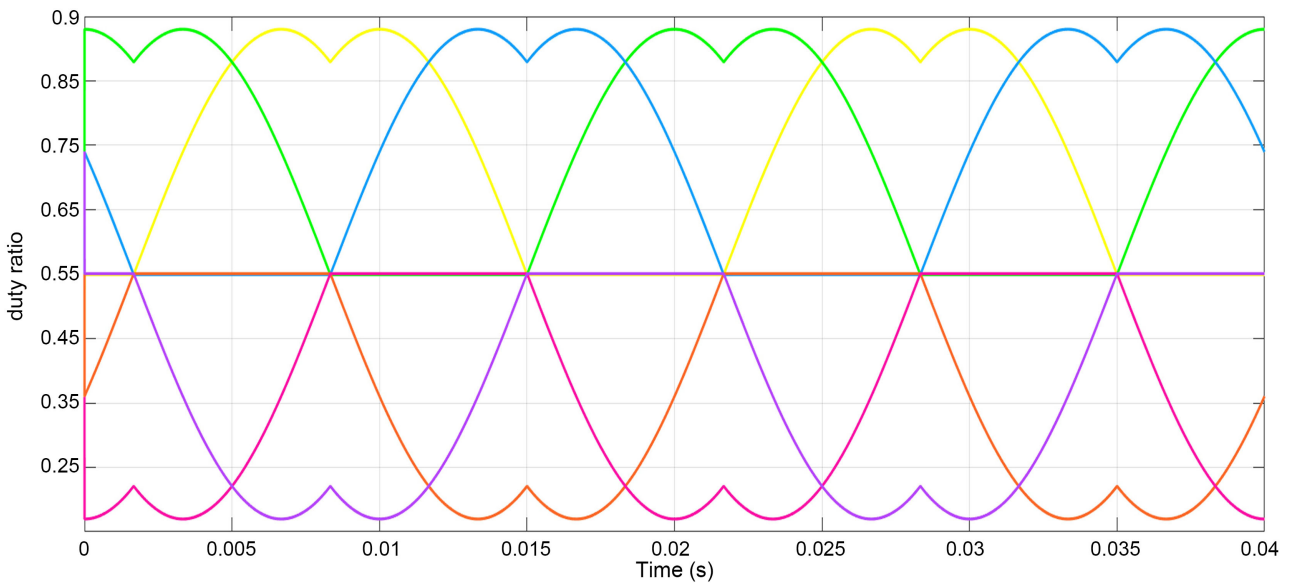


Figure 21. Duty ration.

The duty cycle determines the duration the switch is on, thus influencing the voltage and current of the PV system. Adjusting the duty ratio is essential to maximize energy efficiency by regulating the energy extracted from the solar panel, ensuring that the system operates near its maximum power point (MPP) under varying sunlight conditions. Pulse Width Modulation is used for controlling the voltage of the converters, as shown in **Figure 22**.

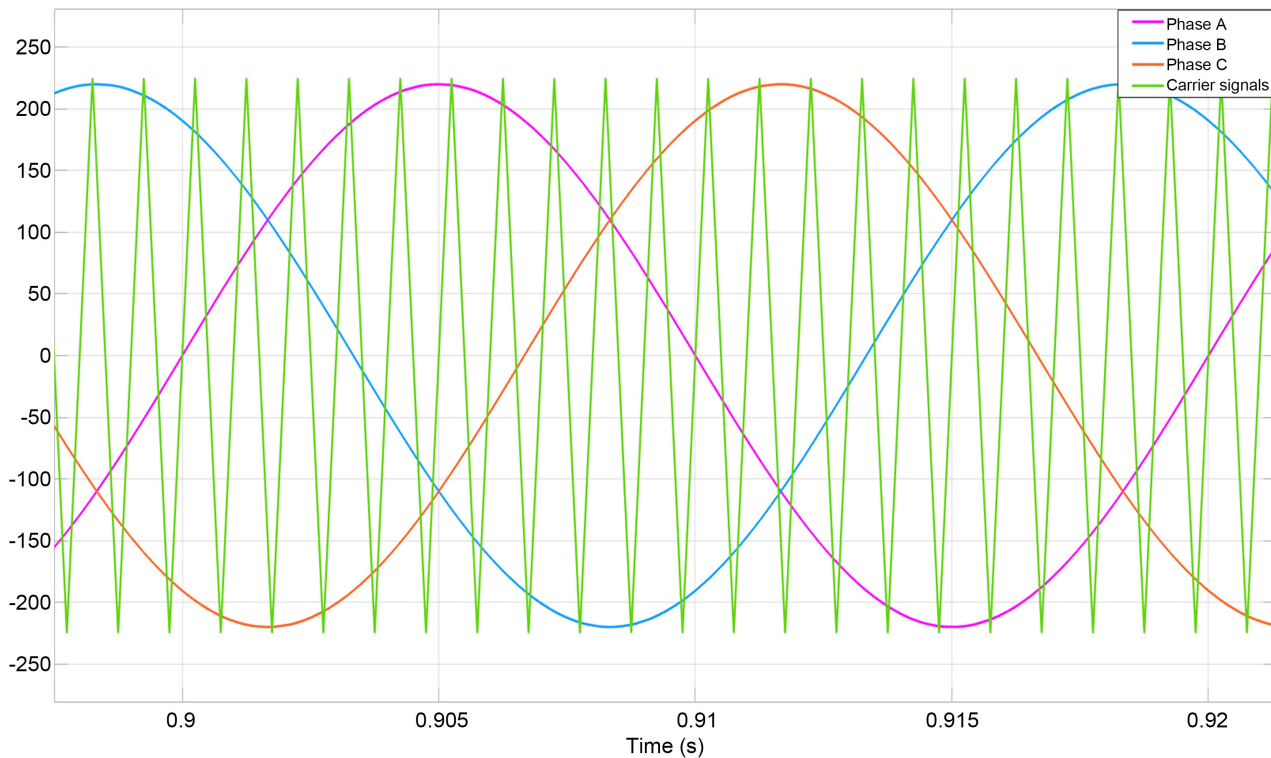


Figure 22. Sine voltage pulse width modulation.

And current of the inverter, which converts the DC power from the solar panels into AC power suitable for the grid or local consumption, as shown in **Figure 22**. SVPWM is particularly advantageous because it helps to minimize harmonic distortion in the output signal, thereby improving power quality. Additionally, by using a sinusoidal reference, the inverter can operate more smoothly and efficiently, which is essential for maximizing the energy yield of solar panels and ensuring the stability of the power system. Adjusting the modulation index allows for precise control of the output voltage, which is especially useful under varying sunlight conditions.

4. Conclusion

A case study has been conducted to highlight certain performance issues of MPPT (Maximum Power Point Tracking). This study presented a representative model of a three-phase photovoltaic system connected to the electrical grid of the Republic of Congo, aiming to stabilize the MPPT. We applied the P&O (Perturb and

Observe) method, while Incremental Conductance compares the attributes of various conventional, significance and novelty of adaptability controller system of the proposed of method and improved incremental conductance algorithms, perturbation and observation techniques, and other maximum power point tracking (MPPT) algorithms in normal and partial shading conditions and observed an improvement in the performance of the grid-connected photovoltaic system. To minimize potential perturbation errors of the P&O algorithm because of the improvement of the incremental conductance algorithm due to rapid irradiation changes also better than P&O algorithm low cost, this paper proposes an enhanced MPPT stabilization and adaptability algorithm on their implementation on Incremental Conductance. Our control scheme uses grid current and the PI signal error to refine the maximum power point tracking. This MPPT method allows for better differentiation of the contribution of the three-phase photovoltaic inverter model connected to the grid. The advantages observed include effective compensation for voltage issues by injecting the maximum power from the PV system into the grid-connected inverter. The fundamental harmonic frequencies are in the range of 0 to 100 Hz, with a total harmonic distortion rate of 11.69%. Although this harmonic distortion rate has been seen high, the P&O (Perturb and Observe) method has proven effective in improving MPPT in the context of connecting a PV-inverter system to the electrical grid of the Republic of Congo.

Conflicts of Interest

The authors declare no conflicts of interest regarding the publication of this paper.

References

- [1] Shimizu, T., Hashimoto, O. and Kimura, G. (2003) A Novel High-Performance Utility-Interactive Photovoltaic Inverter System. *IEEE Transactions on Power Electronics*, **18**, 704-711. <https://doi.org/10.1109/tpel.2003.809375>
- [2] ESRAM, T., Kimball, J.W., Krein, P.T., Chapman, P.L. and Midya, P. (2006) Dynamic Maximum Power Point Tracking of Photovoltaic Arrays Using Ripple Correlation Control. *IEEE Transactions on Power Electronics*, **21**, 1282-1291. <https://doi.org/10.1109/tpel.2006.880242>
- [3] Femia, N., Petrone, G., Spagnuolo, G. and Vitelli, M. (2005) Optimization of Perturb and Observe Maximum Power Point Tracking Method. *IEEE Transactions on Power Electronics*, **20**, 963-973. <https://doi.org/10.1109/tpel.2005.850975>
- [4] Zeng, Q.R. and Chang, L.C. (2005) Improved Current Controller Based on SVPWM for Three-Phase Grid-Connected Voltage Source Inverters. *Power Electronics Specialists Conference*, Dresden, 16 June 2005, 2912-2917.
- [5] Taherbaneh, M. and Menhaj, M.B. (2007) A Fuzzy-Based Maximum Power Point Tracker for Body Mounted Solar Panels in LEO Satellites. 2007 *IEEE/IAS Industrial & Commercial Power Systems Technical Conference*, Edmonton, 6-11 May 2007, 1-6. <https://doi.org/10.1109/icps.2007.4292092>
- [6] Li, P., Zhang, L., Wang, Y. and Sheng, Y.-B. (2008) Research on the Control of the Single-Stage Photovoltaic System in Microgrid. 2008 *China International Conference on Electricity Distribution*, Guangzhou, 10-13 December 2008, 1-7. <https://doi.org/10.1109/ciced.2008.5211660>

- [7] Alonso-Martinez, J., Eloy-Garcia, J. and Arnaltes, S. (2009) Control of a Three-Phase Grid-Connected Inverter for Photovoltaic Application with a Fuzzy MPPT under Unbalanced Conditions. *13th European Conference on Power Electronics and Applications*, Barcelona, 8-10 September 2009, 1-7.
- [8] Carannante, G., Fraddanno, C., Pagano, M. and Piegari, L. (2009) Experimental Performance of MPPT Algorithm for Photovoltaic Sources Subject to Inhomogeneous Insolation. *IEEE Transactions on Industrial Electronics*, **56**, 4374-4380. <https://doi.org/10.1109/tie.2009.2019570>
- [9] Bouchafaa, F., Beriber, D. and Boucherit, M.S. (2010) Modeling and Simulation of a Grid Connected PV Generation System with MPPT Fuzzy Logic Control. *2010 7th International Multi-Conference on Systems, Signals and Devices*, Amman, 27-30 June 2010, 1-7. <https://doi.org/10.1109/ssd.2010.5585530>
- [10] Tey, K.S. and Mekhilef, S. (2014) Modified Incremental Conductance MPPT Algorithm to Mitigate Inaccurate Responses under Fast-Changing Solar Irradiation Level. *Solar Energy*, **101**, 333-342. <https://doi.org/10.1016/j.solener.2014.01.003>
- [11] Sivakumar, P., Abdul Kader, A., Kaliavaradhan, Y. and Arutchelvi, M. (2015) Analysis and Enhancement of PV Efficiency with Incremental Conductance MPPT Technique under Non-Linear Loading Conditions. *Renewable Energy*, **81**, 543-550. <https://doi.org/10.1016/j.renene.2015.03.062>
- [12] Sudhakar Babu, T., Rajasekar, N. and Sangeetha, K. (2015) Modified Particle Swarm Optimization Technique Based Maximum Power Point Tracking for Uniform and under Partial Shading Condition. *Applied Soft Computing*, **34**, 613-624. <https://doi.org/10.1016/j.asoc.2015.05.029>
- [13] Kotti, R. and Shireen, W. (2015) Efficient MPPT Control for PV Systems Adaptive to Fast Changing Irradiation and Partial Shading Conditions. *Solar Energy*, **114**, 397-407. <https://doi.org/10.1016/j.solener.2015.02.005>
- [14] Harrag, A. and Messalti, S. (2015) Variable Step Size Modified P&O MPPT Algorithm Using Ga-Based Hybrid Offline/Online PID Controller. *Renewable and Sustainable Energy Reviews*, **49**, 1247-1260. <https://doi.org/10.1016/j.rser.2015.05.003>
- [15] Verma, D., Nema, S., Shandilya, A.M. and Dash, S.K. (2016) Maximum Power Point Tracking (MPPT) Techniques: Recapitulation in Solar Photovoltaic Systems. *Renewable and Sustainable Energy Reviews*, **54**, 1018-1034. <https://doi.org/10.1016/j.rser.2015.10.068>
- [16] Li, X., Wen, H., Jiang, L., Xiao, W., Du, Y. and Zhao, C. (2016) An Improved MPPT Method for PV System with Fast-Converging Speed and Zero Oscillation. *IEEE Transactions on Industry Applications*, **52**, 5051-5064. <https://doi.org/10.1109/tia.2016.2599899>
- [17] Ling, L., Wu, X.L., Liu, M.Y., Zhu, Z.Q., Li, Y. and Shang, B.B. (2016) Development of Photovoltaic Hybrid LED Street Lighting System. *2016 IEEE Advanced Information Management, Communicates, Electronic and Automation Control Conference (IMCEC)*, Xi'an, 3-5 October 2016, 729-732. <https://doi.org/10.1109/imcec.2016.7867305>
- [18] Loukriz, A., Haddadi, M. and Messalti, S. (2016) Simulation and Experimental Design of a New Advanced Variable Step Size Incremental Conductance MPPT Algorithm for PV Systems. *ISA Transactions*, **62**, 30-38. <https://doi.org/10.1016/j.isatra.2015.08.006>
- [19] Husain, M.A., Tariq, A., Hameed, S., Arif, M.S.B. and Jain, A. (2017) Comparative Assessment of Maximum Power Point Tracking Procedures for Photovoltaic Systems. *Green Energy & Environment*, **2**, 5-17. <https://doi.org/10.1016/j.gee.2016.11.001>

- [20] Dousoky, G.M. and Shoyama, M. (2017) New Parameter for Current-Sensorless MPPT in Grid-Connected Photovoltaic Vsis. *Solar Energy*, **143**, 113-119. <https://doi.org/10.1016/j.solener.2016.12.047>
- [21] Messalti, S., Harrag, A. and Loukriz, A. (2017) A New Variable Step Size Neural Networks MPPT Controller: Review, Simulation and Hardware Implementation. *Renewable and Sustainable Energy Reviews*, **68**, 221-233. <https://doi.org/10.1016/j.rser.2016.09.131>
- [22] Ezinwanne, O., Zhongwen, F. and Zhijun, L. (2017) Energy Performance and Cost Comparison of MPPT Techniques for Photovoltaics and Other Applications. *Energy Procedia*, **107**, 297-303. <https://doi.org/10.1016/j.egypro.2016.12.156>
- [23] Tey, K.S., Mekhilef, S., Seyedmahmoudian, M., Horan, B., Oo, A.T. and Stojcevski, A. (2018) Improved Differential Evolution-Based MPPT Algorithm Using SEPIC for PV Systems under Partial Shading Conditions and Load Variation. *IEEE Transactions on Industrial Informatics*, **14**, 4322-4333. <https://doi.org/10.1109/tii.2018.2793210>